



Research Article

OPTICAL PROPERTIES PYRIMIDINE DERIVATIVES: EFFECT OF ELECTRON-DONOR/ACCEPTOR SUBSTITUENTS IN MOLECULAR TOPOLOGY

Zenaide Severina do Monte ^{1,2}, Leonis Lourenço da Luz ³, Filipe Gabriel Martinez Mauricio ⁴, Ingrid Távora Weber ^{4,5}, Ricardo Oliveira Silva ³, Severino Alves Junior ³, Emerson Peter da Silva Falcão ⁶, Sebastião José de Melo ^{1,2*}

¹ Postgraduate Program in Pharmaceutical Sciences- 50740-560, Recife, PE, Brazil

² Postgraduate Program in Biological Sciences, Federal University of Pernambuco -50740-560, Recife, PE, Brazil

³ Fundamental Department of Chemistry, Federal University of Pernambuco -50740-560, Recife, PE, Brazil

⁴ Materials Science Program, Federal University of Pernambuco - 50740-560, Recife, PE, Brazil

⁵ Inorganic and Materials Laboratory, University of Brasília - 70910-000, Asa Norte, Brasília, DF, Brazil

⁶ Nucleo de Nutrição da Universidade Federal de Pernambuco, Centro Acadêmico de Vitória (CAV), CEP, 55608-680, Vitória de Santo Antão, PE, Brazil

*Corresponding Author Email: melosebastiao@yahoo.com.br.

Article Received on: 15/05/19 Approved for publication: 17/06/19

DOI: 10.7897/2230-8407.1008238

ABSTRACT

In this work, we describe the synthetic approach of pyrimidine-substituted derivatives, photoluminescence properties and theoretical calculations of the geometry optimization and electron density distribution on the molecules in the ground and excited states. According to calculations, the location of HOMO electron density is mainly located over the molecular region with highest electron-donor character (or lower electron-acceptor). On the other hand, the electronic transition from HOMO to LUMO promotes a change in the electron density distribution on the molecule. The simulations also reveal that plane of all aryl substituent's located at positions 2 and 6, are out of the pyrimidine ring plane and the absolute dihedral angles values between n-(p-phenyl) and pyrimidine ring planes are intrinsically dependent on the spatial HOMO distribution on the phenyl ring and p-substituent group. The higher donor character of the substituent leads to substantial changes in the absorption spectra. We also notice that the absorption changes are intrinsically related to the portion of ICT in the molecules, which are strongly dependent on polar interaction. All compounds present large Stokes shifts, higher than 3.370 cm⁻¹, and the emission spectra in solution present broad bands in the ultraviolet-visible region. On the other hand, the solid-state luminescence of 3a and 3c compounds shows emission band in the near-yellow color region 0.423, 0.475 (x, y) and 0.485, 0.542, respectively, in which the 5a and 5c compounds exhibit emission bands corresponding to the near-red color region 0.569, 0.415 and 0.608, 0.389, respectively.

Keywords: Pyrimidines, photophysical properties, theoretical study, effect of electron-donor/acceptor, solvatochromism

INTRODUCTION

Over the years, heterocyclic compounds have received attention in both academic and industry due to their optical and biological properties. Outstandingly, azaheterocycles are known to presents strong aromaticity, significant electron-deficiency, pH sensitivity and capability of nitrogen atoms act in chelation processes, resulting in lower energy band gaps¹⁻³. This characteristic profile proved to be suitable for several applications such as pharmacophore compounds^{4,5}, dyes⁶, organic light emitting diodes (OLEDs)⁷, solar cells⁸, sensor^{1,2,9}, among others. In particular, the pyrimidine ring is frequently reported as strong electron-withdrawing units in donor-acceptor π -conjugated structures (push-pull system) that results in higher optical activities¹⁰. It has long been known that UV-vis/IR optical properties are intrinsically influenced by the chemical environment and different solvent types can bring out changes in position, intensity, and shape of absorption spectra. Solvatochromism studies, in these also called diazo dyes, have indicated bathochromic (positive solvatochromism) and hypochromic (negative solvatochromism) behaviors upon increasing of the solvent polarity. However, experimental and theoretical investigations about solvent-solute interactions are

one of the most difficult tasks, given the interaction complexity involved¹⁰.

In the light of the above mentioned, our work report on the photoluminescence azaheterocycles derivatives series based on a 5-cyanopyrimidines core and 2,4,6-Trisubstituted periphery. Starting from the synthesized molecules are reported in literature¹¹⁻¹³, we decide emphasized the study into two sections. The investigation of optical properties is provided by the electron-deficiency in the pyrimidine ring in front of different substituents. In such a way, theoretical computational methods were used to investigate the bathochromic effect in different solvents.

MATERIALS AND METHODS

The photoluminescence measurements were performed in a spectrofluorometer Horiba-Jobin-Yvon Fluorolog-3 using as excitation source a xenon lamp continuous 450 W xenon lamp and UV xenon flash tube. The detection was made by a Hamamatsu R 928 P photomultiplier. The spectral correction was made by spectral response of the monochromators and using a silicon photodiode reference to monitor and compensate the power output of xenon lamp, using typical correction spectra

provided by the manufacturer. UV-vis absorption measurements were performed in a UV-2600 from Shimadzu.

Molecular orbital and dihedral angles calculations

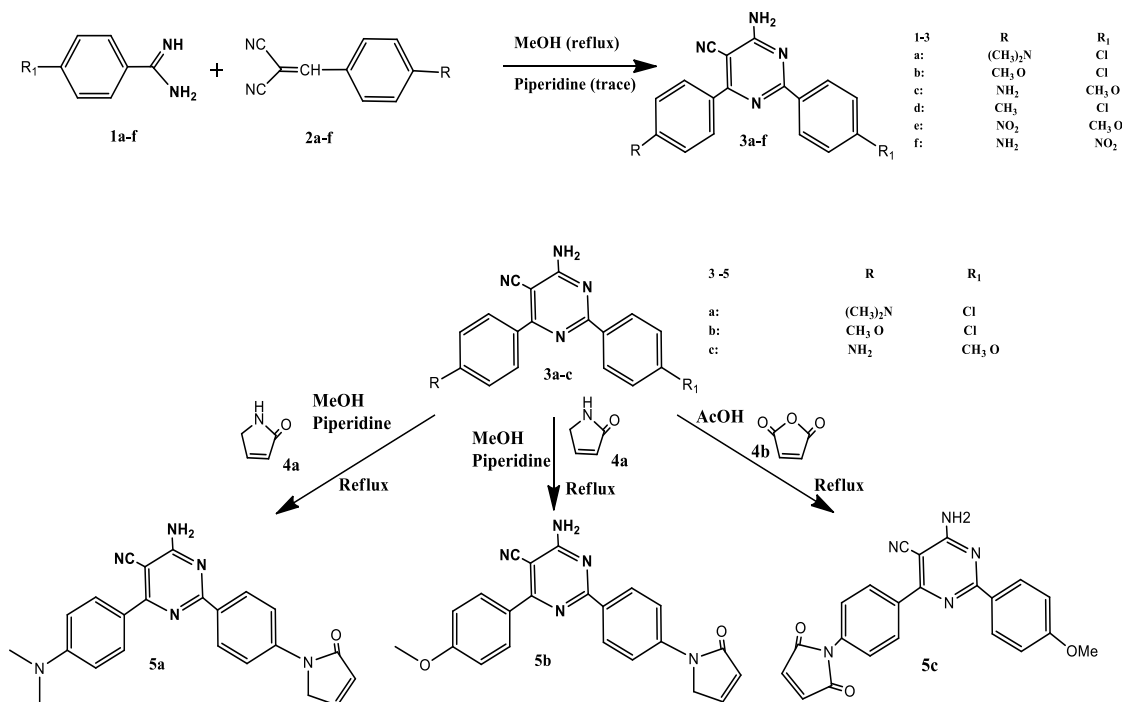
Theoretical calculations of the compounds 3a-f and 5a-c were conducted using semi empirical and Density Functional Theory (DFT). The full geometry optimization was carried out using PM3 Hamiltonian as incorporated in Gaussian 09 package. No symmetry or internal coordinate's constraints were applied during the optimization. The ground states were calculated with the B3LYP functional employing a 6-31G* basis set provided by

Games 64 software package. Additionally, images of HOMO (Highest Occupied Molecular Orbital) and LUMO (Lowest Unoccupied Molecular Orbital) distribution were rendered using Avogadro Software.

RESULTS AND DISCUSSION

Molecular orbital calculations

Nine compounds pyrimidine derivatives¹¹⁻¹³, named as 3a-f and 5a-c, were successfully synthesized using the experimental conditions displayed in Scheme 1.



Scheme 1: Schematic representation of the synthetic approach of compounds 3a-f and 5a-c

To understand better the photophysical properties of the proposed molecules, the optimized molecular geometries and, frontier molecular orbital energy diagram and location were calculated, and the results displayed in Figures 1. The electron donating effect were investigated for the p-substituents in the n-(p-phenyl) groups in the positions 2 and 6 of pyrimidine center; could be noted that the HOMO electron density is mainly located over the molecular region with highest electron-donor character (or lower electron-acceptor). The electronic transition from HOMO to LUMO, or vice versa, promotes a change in the electron density distribution on the molecule, relatively to HOMO distribution. In this context, we notice three different orbital behaviors in our simulations: The

first one, both HOMO and LUMO presents electron density distribution fullest extended over the molecule induced by chloride substituent, as seen to the 3a, 3b and 3d molecules. For second, HOMO is mainly located above of p-phenyl substituent whereas LUMO distribution extends mainly over the pyrimidine ring. This behavior was observed for 3c, 5a and 5b. On the third one, HOMOs are located over a region opposite and distinct from the LUMO region. This could be observed in Figure 1(e) e and 1(i), which shows HOMO located over the p-phenyl containing the group with the lowest electron-acceptor character. In another hand, LUMO appears under the 6-(p-phenyl) substituent.

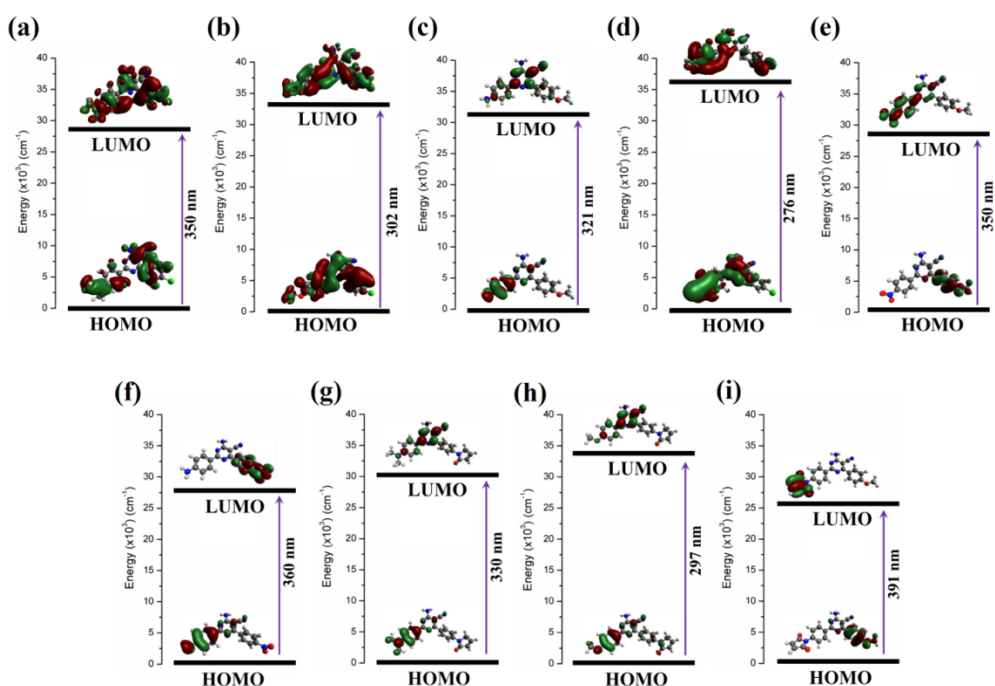


Figure 1: Calculated spatial distributions of frontier molecular orbital (HOMO and LUMO) and their energy gap for 3a-3f (a-f), and 5a-5c (g)-(i) molecules

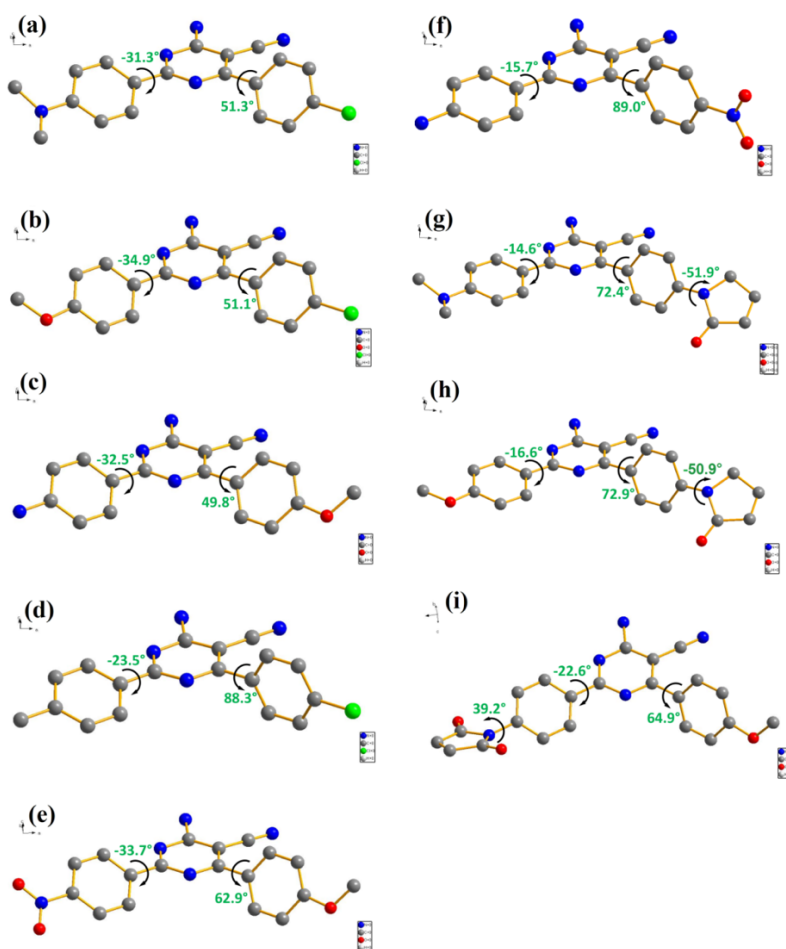


Figure 2: Absolute dihedral angles for 3a-3f (a)-(f), and 5a-5c (g)-(i) molecules

The simulations also reveal that all aryl substituents, located at positions 2 and 6, are out of pyrimidine ring plane. We observed that the absolute dihedral angles values (Figure 2), correlated with *n*-(*p*-phenyl) and pyrimidine ring planes (Figure 3) are intrinsically dependent of the spatial HOMO distribution on the *p*-phenyl, mainly on the *p*-substituent group. Further, lower dihedral angle was observed in the range of 14.6° until 34.9° and corresponds to the molecular region which the HOMO is predominantly located. In a surprising way the 2-(*p*-phenyl) position shows lower torsion angles for all compounds. In contrast, the highest dihedral angles, ranging from 49.8° to 89.0°,

were related to the 6-(*p*-phenyl) position that clearly suffers distortion influence from the 5-carbonitrile electron density. It's should be the point that the small dihedral angles for 5a (14.6°), 3f (15.7°) and 5b (16.6°) molecules at position 6 of pyrimidine ring exhibit a systematic dependence of character donor-acceptor and electro negativity of *p*-substituents. Moreover, dihedral angles between 6-(*p*-phenyl) and *p*-pyrrolone moieties (in 5a and 5b) show both similar values 51.9° and 50.9°, respectively, while the maleimide moieties and 2-(*p*-phenyl) presents a torsion angle of 39.2° in the 5c molecule.

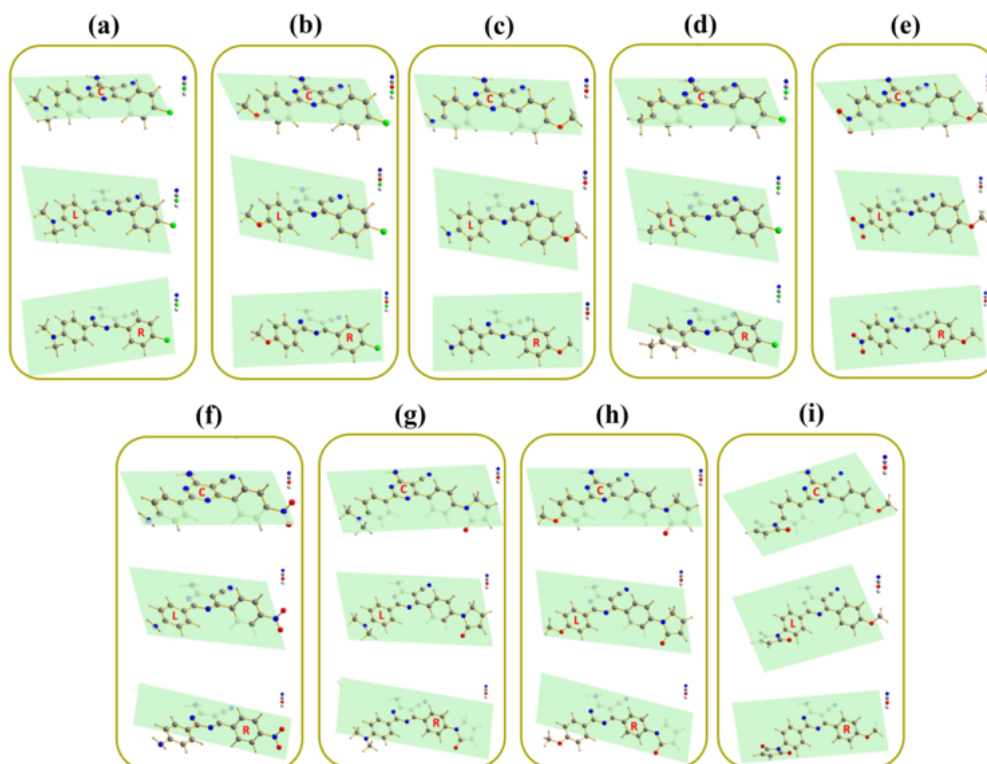


Figure 3: Representation of plane of ring to 2(*p*-Phenyl) (Left), 6(*p*-Phenyl) (Right) and Pyrimidine (Central) rings of the 3a-3f (a)-(f), and 5a-5c (g)-(i) molecules

To investigate the molecular energy involved, when comparing the energy gap between HOMO and LUMO we observed that electron-donor substituent in 2-(*p*-phenyl), aligned with the electron-acceptor an isil group at position 6, promotes a higher stabilization of molecule in detriment to other substituents. These trends are in agreement with the behavior observed to 5a and 5b molecules. As a fore mentioned, shows a strong dependence of molecular orbital distribution and energy gap between HOMO-LUMO with nature electron-donor/acceptor of the substituent at position 6 of the pyrimidine ring. This behavior, until then unusual with typical pyrimidine derivatives, can be explained mainly by the presence of amino and cyano groups at positions 4 and 5 of the pyrimidine ring, respectively, that affect their electron-acceptor character.

Optical properties

The experimental photophysical properties were performed for the pyrimidine derivatives 3a, 3c, 5a and 5c in solution and solid state, at room temperature. Their absorption and emission spectra in methanol, ethanol, acetonitrile, chloroform and dichloromethane were displayed in Figures 6 and 7, besides that the corresponding spectroscopic data are summarized in Table 1. The absorbance spectra of 3a, 3c, 5a and 5c compounds were obtained by UV-visible absorption spectroscopy. Considering the HOMO→LUMO transitions, the first absorption bands in the spectra of 3c and 5a could be associate to π - π^* and intra molecular charge transfer (ICT) transition, while the 3a presents only an ICT transition and 5 π - π^* transitions. That information is in agreement with the magnitude of the molar extinction coefficients of the lowest energy band (ϵ) in Table 1.

Table 1: Photophysical data of 3a, 3c, 5a and 5c in different solvents at room temperature

Compound	Solvent	Absorbance		Emission λ_{Max}^a/nm	Stokes shift/cm ⁻¹
		λ_{Max}^a/nm ($\epsilon^a/10^4M^{-1}cm^{-1}$)	λ_{Max}^b/nm ($\epsilon^b/10^4M^{-1}cm^{-1}$)		
3a	Methanol	340 (1.1)	296 (1.5)	384	3.370
	Ethanol	342 (1.2)	298 (1.5)	414	5.085
	Acetonitrile	338 (1.4)	297 (1.6)	- ^d	- ^d
	Chloroform	343 (1.6)	302 (1.3)	- ^d	- ^d
	Dichloromethane	341 (1.6)	301 (1.5)	- ^d	- ^d
3c	Methanol	345 (2.6)	279 (1.0)	410	4.595
	Ethanol	346 (1.7)	277 (0.9)	420	5.092
	Acetonitrile	329 (0.2)	274 (0.8)	- ^d	- ^d
	Chloroform	332 (0.2)	270 (1.0)	- ^d	- ^d
	Dichloromethane	327 (0.1)	271 (0.7)	- ^d	- ^d
5a	Methanol	335 (1.1)	275 (5.0)	460	8.112
	Ethanol	337 (0.8)	276 (3.8)	455	7.696
	Acetonitrile	332 (0.9)	276 (3.7)	- ^d	- ^d
	Chloroform	332 (1.0)	280 (3.8)	- ^d	- ^d
	Dichloromethane	331 (1.0)	280 (3.2)	- ^d	- ^d
5c	Methanol	302 (0.9)	257 (3.6)	360	5,335
	Ethanol	321 (0.2)	254 (1.5)	415	7,056
	Acetonitrile	- ^c	258 (0.4)	- ^d	- ^d
	Chloroform	- ^c	257 (0.2)	- ^d	- ^d
	Dichloromethane	- ^c	256 (0.4)	- ^d	- ^d

- a. First excited state (lowest-energy absorption maximum); a'. maximum fluorescence excited at the lowest-energy absorption maximum;
 b. Second excited state; c. Not detected due to very weak emission; d. No were performed

The 3c and 5c compounds exhibit different spectral profiles due to changing of solvent. We notice that protic solvents are responsible for large changes in absorption which indicate a strong sensitivity of the donor groups. In contrast, the 3a and 5a compounds (Figure 1 and 3) do not present significant alterations in face to increase of solvent polarity. This behavior was correlated with the p-substituent type and their solvent interactions (hydrogen bond and/or dipole-dipole), which shows a large dependence of the character donor-acceptor in 6-(p-phenyl). In this way, higher donor character of the substituent, lead to substantial changes on the absorption spectra, as seen in Figure 3. We also notice that the absorption changes are intrinsically related to the portion of ICT in the molecules, which is strongly dependent of polar interaction. This behavior could be associated with 3c and 5c molecules. On the basis of the behavior of the 5a

(Figure 3), we suggest that the mechanism involved in $\pi \rightarrow \pi^*$ transition is most pronounced. This induces 5a to a similar behavior observed for 3a molecule, in which the ICT mechanism is absent. Table 1, 3c and 5c show systematic decrease of ϵ face to the reduction of solvent polarity. It is seen to 3c molecule a remarkable decrease from 1.7×10^4 (ethanol) to $0.2 \times 10^4 L.M^{-1}.cm^{-1}$ (acetonitrile), whereas in 5c is from $0.2 L.M^{-1}.cm^{-1}$ (ethanol) to non-detected (acetonitrile). Moreover, 3a exhibit a slight growth of ϵ , rising from 1.1×10^4 (methanol) to $1.6 \times 10^4 L.M^{-1}.cm^{-1}$ (dichloromethane). This behavior is associated with the above-mentioned mechanism and the molecular localization of the frontier orbitals. The 5a molecule does not present a trend in the ϵ profile, probably correlated with an oscillation between the electronic transition mechanisms (ICT and $\pi \rightarrow \pi^*$), as mentioned before.

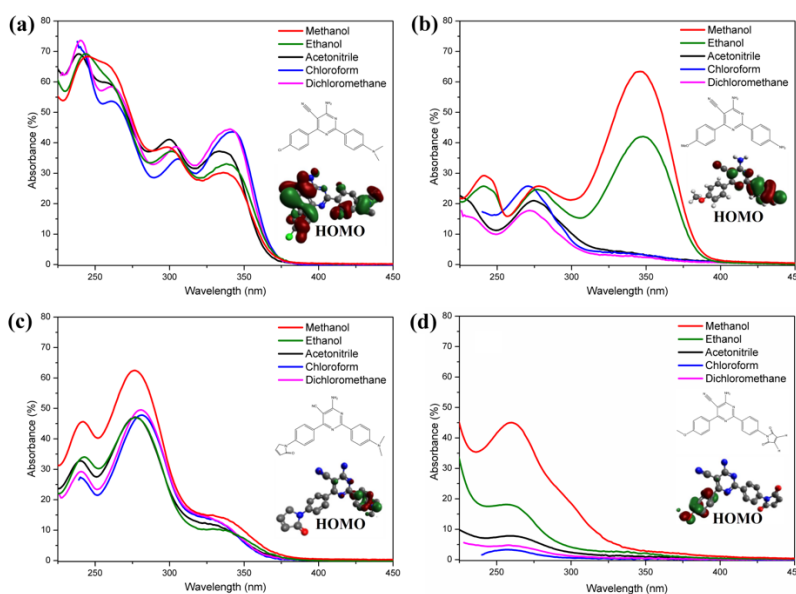


Figure 4: UV-visible absorption of 3a (a), 3c (b), 5a (c) and 5c (d) ($[C] = 1.25 \times 10^{-5} \text{ M}$) in methanol, ethanol, Acetonitrile, chloroform and dichloromethane at room temperature

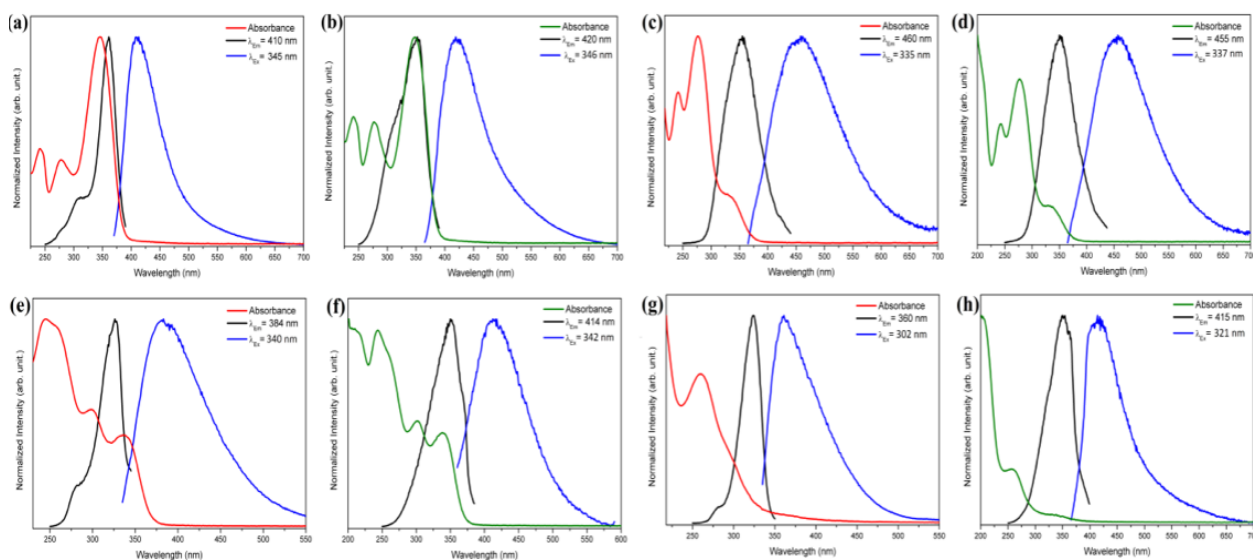


Figure 5: Normalized absorption (red and green line), excitation (black line) and emission (blue line) spectra of 3a in methanol (a) and ethanol (b), 3c in methanol (c) and ethanol (d), 5a in methanol (e) and ethanol (f), and 5c in methanol (g) and ethanol (h)

In Figure 6, we investigated the optical properties of compounds 3a, 3c, 5a and 5c in methanol and ethanol using photoluminescence spectroscopy. The emission spectra of all molecule's present broad bands in the ultraviolet-visible region (UV-vis) with maximum centered peaks ranging from 360 to 460 nm. The excitation spectra were acquired by monitoring emission at the maximum of emission and emission spectra was performed by exciting at a maximum of the first absorption band (Table 1). The absence of fell high energy absorption bands in excitation spectra in all molecules suggests a higher incidence of non-

radioactive process, promoting a deactivation of the molecular electronic excited states by mechanisms such molecular collision, cross-relaxation, among others¹⁴. All molecules present large Stokes shifts, higher than 3.370 cm^{-1} (Table 1). The 3a presents the lowest value that was associated to the low stabilization of the molecular excited state by the solvent, furthering the observed shift. On the other hand, 5a compound shows the higher values of Stokes shift (8.112 cm^{-1} -methanol and 7.696 cm^{-1} - ethanol) and presents the large stabilization for polar solvents in the excited state (Figure 1, Table 1 and Figure 6).

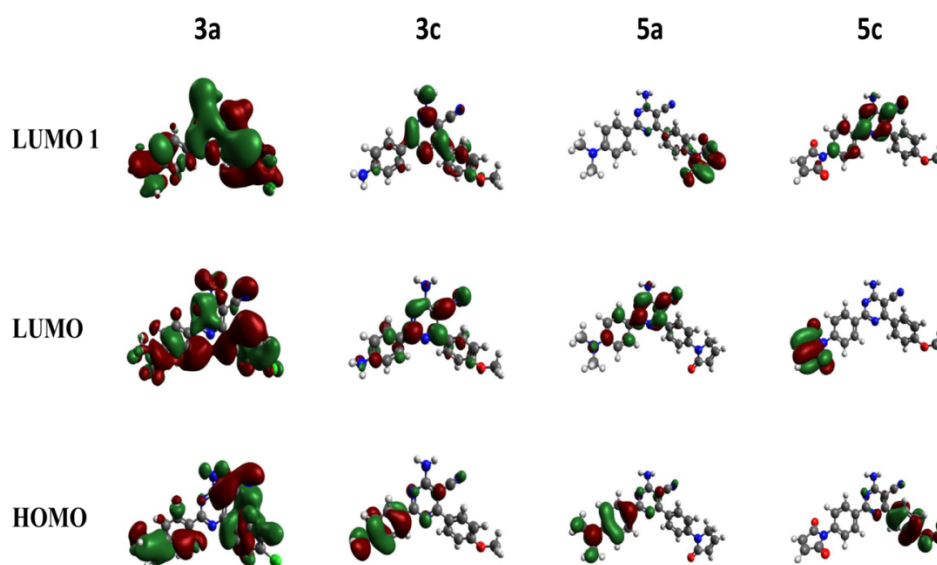


Figure 6: Electron density distribution of HOMO, LUMO and LUMO 1 of the 3a,c and 5a,c molecules

Also, should be noted that the shift values are more prominent for samples measured in ethanol, this because the interactions of LUMO electronic orbitals with the hydrophobic group on solvent molecules leads to a better stabilization effect. In contrast, 5a shows a disparate behavior once that the LUMO distribution allows H-bond interactions with the OH group of the solvent, increasing the stability effect. In Figure 7, the solid-states spectroscopic measurements show lower band gap values in the excited state than the samples in the solvent. Excitation spectra were recorded by monitoring emission at 550, 580, 610 and 600 nm, respectively to 3a, 3c, 5a and 5c molecules. Emission spectra of 3a, 3c, 5a and 5c molecules were performed by excitation at 435, 405, 465 and 515 nm, respectively. The samples 3a and 3c shows emission band in the near-yellow color region and presents the respective color coordinates 0.423, 0.475 and 0.485, 0.542 (x, y) in the chromaticity diagram coordinate in accordance with International Commission of Illumination (CIE) in 1931. Moreover, 5a and 5c compounds exhibit an emission band corresponding to the near-red color region and CIE coordinates as 0.569, 0.415 and 0.608, 0.389, respectively. This change in the photoluminescence color between 3a, c and 5a, c materials are correlated to increased conjugated π bonds with the change of p-substituent.

CONCLUSION

The investigation of the effect of electron donates groups at the positions 2 and 6 of the n-(p-phenyl) ring reveal that the HOMO electron density is mainly located over the molecular region with highest electron-donor character (or lower electron-acceptor). On the other hand, the electronic transition from HOMO to LUMO promotes a change in the electron density distribution on the molecule. The simulations also reveal that all planes of aryl

substituents, located at positions 2 and 6, are out of the pyrimidine ring plane. We observed that the absolute dihedral angles values between n-(p-phenyl) and pyrimidine ring planes are intrinsically dependent on the spatial HOMO distribution on the phenyl ring and p-substituent group. It is worth pointing that the small dihedral angles for 5a (14.6°), 3f (15.7°) and 5b (16.6°) molecules at position 6 of pyrimidine ring exhibit a systematic dependence of character donor-acceptor and electro negativity of p-substituents. Comparing the energy gap between HOMO and LUMO we observed that electron-donor substituent in 2-(p-phenyl), aligned with the electron-acceptor anisil group at position 6, promotes a higher stabilization of molecule in detriment to other substituents. The higher donor character of the substituent, leads to substantial changes in the absorption spectra, as seen in Figure 3. We also notice that the absorption changes are intrinsically related to the portion of ICT in the molecules, which are strongly dependent on polar interaction. However, we suggest that this mechanism involved $\pi \rightarrow \pi^*$ transition is most pronounced. All compounds present large Stokes shifts, higher than 3.370 cm^{-1} , and their emission spectra present broad bands in the ultraviolet-visible region. Also, the shift values are more prominent for samples measured in ethanol due to the interactions of LUMO electronic orbitals with the hydrophobic groups which solvent molecules leads to a better stabilization effect. The solid-state luminescence of 3a and 3c compounds shows emission band in the near-yellow color region 0.423, 0.475 (x, y) and 0.485, 0.542, respectively, in which the 5a and 5c compounds exhibit emission bands corresponding to the near-red color region 0.569, 0.415 and 0.608, 0.389, respectively. This change in the photoluminescence color between 3a, c and 5a, c materials are correlated to increased conjugated π bonds with the changing of p-substituent.

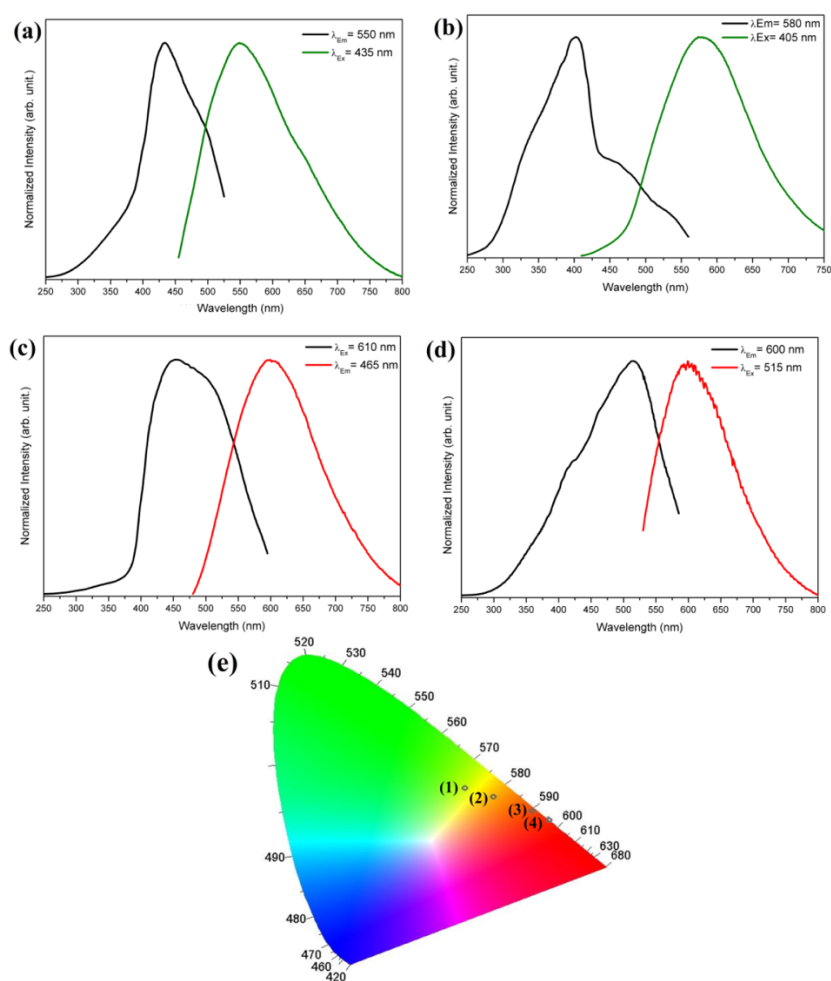


Figure 7: Normalized excitation (black line) and emission (green and red line) spectra of 3a (a), 3c (b) and 5a (c) and 5c (d) in solid state, and chromaticity diagram (e) with corresponding color coordinates of 3a (1), 3c (2) and 5a (3) and 5c (4)

ACKNOWLEDGEMENTS

The authors gratefully acknowledge the Brazilian Agencies FACEPE, CNPq, CAPES, and FINEP for providing financial support under grants: FACEPE/BFP-0094-4.03/17, CNPq/INCT-INAMI -57.3986/2008-8, Pronex APQ-0675-1.06/14, INCT-NANOMARCS APQ-0549-1.06/17, and CNPq process 428020/2016-0. Z.S. do Monte thanks to the Postgraduate Program in Pharmaceutical Sciences and Postgraduate Program in Biological Sciences Chemistry Graduate Program at UFPE and FACEPE and, CNPq/INCT-INAMI fellowships. L. L. da Luz thanks to the Chemistry Graduate Program at UFPE and, FACEPE and PNPd-CAPES fellowships.

REFERENCES

- Nourah ZA, Sheena YM, Yohannan C, Ibrahim PA, Al Swaidan A, El Emam AO Al-Deeb, A Al-Saadi, AA Christian, VA WAR., JA. Spectroscopic investigation (FT-IR and FT-Raman), Vibrational assignments, HOMO-LUMO, NBO, MEP analysis and molecular docking study of 2-[(4-chlorobenzyl)sulfanyl]-4-(2-methylpropyl)-6-(phenylsulfanyl)-pyrimidine-5-carbonitrile, a potential chemotherapeutic agent. *Spectrochimica Acta Part A: Molecular and Bio molecular Spectroscopy* 2015; 139: 413-424.
- Sun SS, Dalton LR. (b) Brabec C, Scherf U, Dyakonov V. *Organic photovoltaics: materials, device physics, and manufacturing technologies*. 1st. Wiley-VCH 2008; 29: 936.
- Smith J, Knasinski SNV, Simmons W, Bhavnani S Ambrose, P, Andes, D. Voriconazole therapeutic drug monitoring. *Antimicrob Agents Chemother* 2006; 50: 1570-1572.
- Ablajan K, Kamil W, Tuoheti A, Wan-Fu S. *Molecules* 2012; 17: 1860.
- Eicher T, Hauptmann S. *The chemistry of heterocycles structure, reactions, syntheses and applications*. 2° ed., Wiley-UCH; 2003.
- Chen PC, Wang IJ. Synthesis and solvatochromic properties of some disazo dyes derived from pyrazolo [1,5-a]pyrimidine derivatives. *Dyes and Pigments* 2005; 64: 259-264.
- Achelle S, Rodríguez-L, J Bure, F Robin-le, FG. Dipicolylaminestyryldiazine derivatives: Synthesis and photophysical studies. *Dyes and Pigments* 2015; 12(1): 305-311.
- Verbitskiy EV, Cheprakova EM, Subbotina JO, Schepochkin AV, Slepukhin PA, Rusinov GL, Charushin VN, Chupakhin ON, Makarova NI, Metelitsa AV, Minkin VI. Synthesis, spectral and electrochemical properties of pyrimidine-containing dyes as photo sensitizers for dye-sensitized solar cells. *Dyes and Pigments* 2014; 100: 201-214.
- Skardziute L, Dodonova J, Voitechovicus A, Jovaisaite J, Komskis R, Voitechovicute A, Bucevicus J, Kazlauskas K, Juršenas S, Tumkevicus S. Synthesis and optical properties of the isomeric pyrimidine and carbazole derivatives: Effects

- of polar substituents and linking topology. *Dyes and Pigments* 2015; 118: 118–128.
10. Raposo MMM, Sousa, AMR, Fonseca, CAM, Kirsch CG. Thienylpyrrole azo dyes: synthesis, solvatochromic and electrochemical properties. *Tetrahedron Letters* 2005; 61(34): 8249-8256.
 11. Do Monte ZS, Monteiro MRL, Borba CBA, De Gusmão NB, Falcão EPS, Silva RO, Srivastava RM, De Melo SJ. Synthesis of 4-amino-2,6-diaryl-5-cyanopyrimidines as antimicrobial agents. *Synthetic Communications* 2016; 46 (11): 983-991.
 12. De Melo, SJ, Do Monte ZS, Da Silva Santos, AC, Silva ACC, Ferreira LFGR, Hernandez MZ, Silva RO, Falcão EPS, Brelaz-de-Castro, MC A, Srivastava RM, Pereira VR, A. Synthesis, anti trypanosomal activity and molecular docking studies of pyrimidine derivatives. *Medicinal Chemistry Research* 2018; 27: 2512-2522.
 13. Melo SJ, Monte ZS, Srivastava RM, Falcão EPS, Silva RO. Heterociclos pirimidínicos potencialmente bioativos e respectivo processo de obtenção e elucidação estrutural. BR 10 2017 0151280. Instituto Nacional de Propriedade Intelectual, Universidade Federal de Pernambuco. Patente de Invenção (PI) 2017; 14: 06.
 14. Natalia GZ, Shawn H, Haiying Z, David MK Mikhail, YB. Minimization of self-quenching fluorescence on dyes conjugated to bio molecules with multiple labeling sites via asymmetrically charged NIR fluorophores. *NIH Public Access* 2014; 9(5): 355-362.

Cite this article as:

Zenaide et al. Optical properties pyrimidine derivatives: Effect of electron-donor/acceptor substituents in Molecular Topology. *Int. Res. J. Pharm.* 2019; 10(8):5-13 <http://dx.doi.org/10.7897/2230-8407.1008238>

Source of support: Brazilian Agencies, Conflict of interest: None Declared

Disclaimer: IRJP is solely owned by Moksha Publishing House - A non-profit publishing house, dedicated to publish quality research, while every effort has been taken to verify the accuracy of the content published in our Journal. IRJP cannot accept any responsibility or liability for the site content and articles published. The views expressed in articles by our contributing authors are not necessarily those of IRJP editor or editorial board members.